The International Journal of Advanced Manufacturing Technology (2019) 101:2907–2922
https://doi.org/10.1007/s00170-018-3134-z

ORIGINAL ARTICLE

Development and characterisation of secured traceability tag for textile products by printing process

Tarun Kumar Agrawal [1,2,3,4] · Christine Campagne [1,2] · Ludovic Koehl [1,2]

Received: 2 August 2018 / Accepted: 22 November 2018 / Published online: 13 December 2018

Abstract

Product security is one of the major concerns in the textile industry. Every year, fashion brands suffer significant loss due to counterfeit products. Addressing this, the paper introduces a secured tag for traceability and security of textile products. The proposed tag is unclonable, which can be manufactured using conventional screen-printing process. Further, it can be read using a smartphone camera to authenticate the product and trace its history. Consequently, imparting additional functionality to the textile through surface modification. To validate its applicability, the study experimentally investigates the durability and readability of the developed secured tag using three different binders on polyester and cotton textiles substrates. A comparison is presented with an in-depth analysis of surfaces and binders interaction at different stages of the secured tag lifecycle, i.e. before print, after print, after wash and after abrasion cycles. The methodology and findings of the study can also be useful for other manufacturing domains dealing with the printing process.

Keywords Secured tag · Traceability · Screen printing · Adhesion

1 Introduction

Textile or clothing that is specifically engineered in order to deliver a predefined functionality or performance to the consumer, in addition to its normal functions is usually termed as 'Functional textile' or 'Functional clothing'. Based on the additional functionality, these textile can be classified as protective-, medical-, sports-, vanity- and cross-functional [1]. Typically made by modifying the textile structure at different scales or adding auxiliary textile assemblies, these functional textiles are flexible and low-cost as compared to conventional non-textile substitutes (e.g. [2, 3]). The additional functionality is usually incorporated at the raw material stage or during manufacturing process [4].

Surface mounting or modification through printing process is one of the most commonly used technique to fabricate supple and inexpensive functional textiles [5–7]. Printing usually transforms or modifies the surface properties for additional functionality and finds wide application in the electronics industries for developing printed sensors, flexible displays, RFIDs and wearable electronics [8–12]. A significant research has focused in past to develop interactive, smart and functional textiles through printing processes [13]. Screen-printing, inkjet printing and 3D printing are some of the well-known technologies used in past to impart various functionalities to textiles [8, 11, 14, 15]. Nonetheless, every technology has its pros and cons. For instance, screen-printing has low infrastructure investment and high deposition. However, it offers lower precision, limited variety and versatility. Inkjet printing, on the other hand, has higher precision, controlled deposition, high productivity and thin-layer deposition capability. Though, it is comparatively expensive, less resistant to bending and stretch and offers high surface roughness [16]. 3D printing, on the other hand, has even higher deposition (in three dimensions) but lower productivity due to its non-continuous process and requires higher infrastructure investment [17]. Overall, compared to

✉ Tarun Kumar Agrawal
Tarun_kumar.agrawal@hb.se; tarun-kumar.agrawal@ensait.fr; tarunagraw@gmail.com

[1] ENSAIT, GEMTEX – Laboratoire de Génie et Matériaux Textiles, 59000 Lille, France

[2] Université Lille Nord de France, 59000 Lille, France

[3] The Swedish School of Textiles, University of Boras, 501 90 Boras, Sweden

[4] College of Textile and Clothing Engineering, Soochow University, Suzhou, China

other manufacturing technologies, these printed functional textiles usually face substantial challenges in the commercial market due to low-durability. Functional ink or paste used for printing are often eroded or washed-off due to low surface affinity. However, with technological advancement and in-depth analysis of the surface-to-surface interaction between printing paste/ink and textile substrates, it is possible to overcome these challenges and develop commercially viable products [18].

Printed traceability tag is one such example which is a widely recognised and accepted technology in the market [19–22]. These tags act as a unique identifier that links product with the central database and enables traceability in the complex supply chain. Printed RFIDs and barcodes are commonly used solutions for high-volume track and trace applications in pharmaceutical, food and logistics industries [23–26]. Though numerous studies in past have advocated the use of RFIDs in the T&C supply chain, consumers perceive them as a threat to privacy due to its hidden and remote readability feature [27]. In addition, RFIDs, QR code and barcode are easily clonable and often detachable, leading to product loss or replacement with counterfeits in the complex supply chain [28]. Nonetheless, when integrated directly on textile products along with an authentication mechanism, these traceability tags can remain integrated to the product, enabling brand authentication and traceability (communicating history of the product) throughout the lifecycle [22]. As a result, it imparts additional functionality to the textile through surface modification. Therefore, the printed tag—that can track and trace the product in the supply chain and secures it from counterfeit threat—are high in demand for the T&C supply chain. These tags are also expected to be durable, inexpensive and eco-friendly [28]. They should safeguard user privacy by restricting remote readability. Besides, these tags should be easily readable and authenticable by the customer in order to access traceability information. They can even be used for sorting and segregation of textile material during recycling stage [29].

In this context, the current study presents a new secured tag for textile product authentication and traceability. The secured tag is unique for each product and extremely hard to replicate. It can be read and verified using a smartphone camera to authenticate the product and trace its history. The functionality in the secured tag is not solely due to printing material and mechanism, but it is a combination of the system developed during the study. It consists of a secured tag that is printed on the textile substrate plus the developed algorithms that read, encode and validate the secured tag using image processing and pattern recognition tool. In order to demonstrate the development process of the secured tag, a systematic approach has been followed. The study explains the concept and manufacturing process, followed by an in-depth analysis of various sourced materials and their interaction to determine the optimum combination that can result in a higher durable and readable secured tag. The parts of the paper are arranged in following order: Section 2 describes the security mechanism and its manufacturing process of the secured tag. Section 3 defines various raw material selected for secured tag manufacturing followed by overview of methods used for material characterisation and secured tag durability and readability analysis. Section 4 discusses the results from various characterisation and analysis and ranks different secured tag samples. Finally, Section 5 summarises the outcome of the study and lists the scope for future research.

2 Concept and manufacturing process

2.1 Concept

The secured tag is inspired by a physical unclonable function (PUF), which is a well-known security mechanism, acting as a

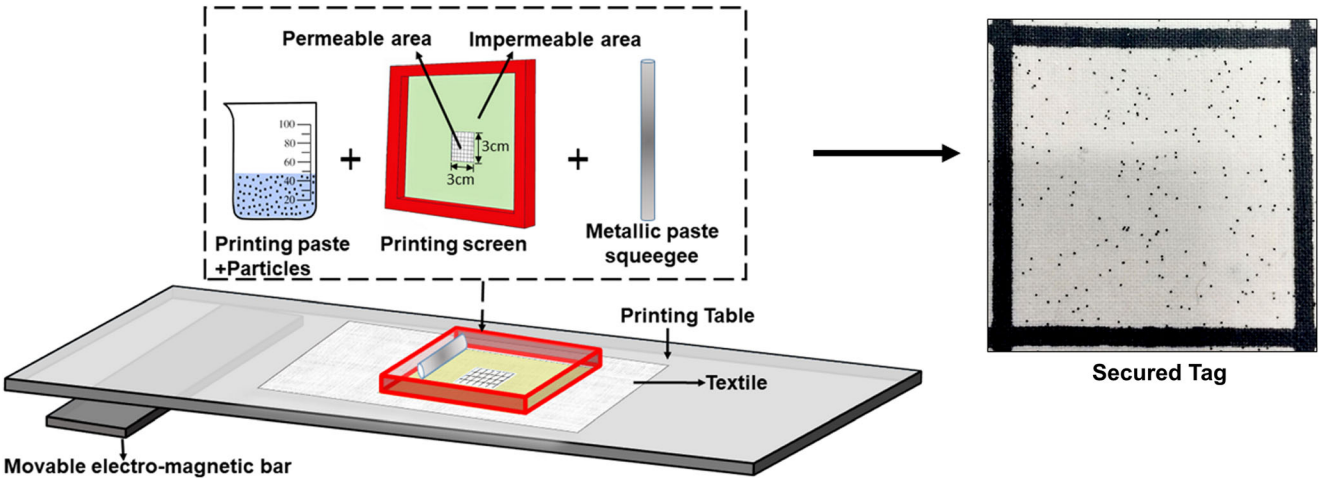

Fig. 1 Electromagnetic printing table with printing tools and image of the developed secured tag

Table 1 Properties of different binders

	Binder 1	Binder 2	Binder 3
Commercial name	Tubvinyl 235 MC® [32]	Silbione TCS 7541® A [33]	Helizarin ET Plus liq® [34]
Chemical nature#	Vinyl acrylic copolymer	Polydimethylsiloxane (silicones)	Styrene acrylic coplomyer
Supplier	CHT Bezema (France)	Blue star silicones (France)	Archroma (France)
Catalyst/fixing agent#	Tubassist® Fix 102 W (3% *w*/*w*)	Silibione TCS® 7604 C (10% *w*/*w*)	Luprintol® Fixing Agent SE liq (1% *w*/*w*)
Glass transition temperature (Tg) (approx.)#	− 19 °C	− 120 °C	+ 5 °C
Solids content (approx.)#	59%	100%	38%
Viscosity – Brookfield (10 rpm) (approx.)*	150,000 mPa.s (needle no°7)	35,000 mPa.s (needle no°6)	140,000 mPa.s (needle no°7)
Curing temperature*	150 °C	150 °C	150 °C
Curing time*	5–6 min	2–3 min	5–6 min

Information source: # Supplier, *Experiment

digital fingerprint for each associated product. PUFs are easy to evaluate and encode but hard to replicate and breach. PUF mechanism taps and records certain innate, uncontrolled and random variation in each product developed during the fabrication process and makes them a unique identifier for that particular product [30]. The proposed tag is secured from reproduction or cloning (that can result in a counterfeit product) through the same concept of PUF and randomness. Each textile product is printed with a micro-level size of the particle through an uncontrolled process, in a confined tag area (3 × 3 cm^2) with varying particle concentration and distribution. This generates a unique particle randomness on each product with a very low probability of reconstruction. This unique randomness acts like a signature for each product that is extremely hard to replicate. These microparticles are detectable through camera images; therefore, the distribution can be extracted and encoded by the manufacturer (using image processing and pattern recognition methods). After the sale, the consumer can validate the product using smartphones to authenticate and trace its history thus promoting transparency and traceability in the T&C supply chain. A detail description of the algorithm and secured tag technology can also be found in our previous work [31]. Likewise, based on the design of garment or textile product, the secured tag can be placed externally and make it an aesthetic feature or internally at a safe location that would not undergo extensive wear and tear. For instance, it can be printed internally, on the yoke or moon patch, just below the brand labels.

2.2 Manufacturing process of the secured tag

The secured tag is manufactured through the screen-printing method. The process uses a porous mesh, commonly known as a screen for the printing process. The printing area or motif acts like a stencil—developed by blocking all the pores of the non-printing area. While printing, the paste (consisting mainly of a binder mixed with a colourant) is squeezed through this stencilled screen onto the textile substrate, thus creating the motif on the textile surface. The print is then dried and cured to harden the paste by cross-link with the textile substrate.

In this study, the printing paste consists of microparticles mixed with a transparent binder, without any colourant. When the mesh screen is placed on the textile substrate and printing paste is squeezed, the microparticles passes through porous part of the mesh and are randomly placed on surface of the textile substrate. To maintain a uniform squeezing pressure, a semi-automatic magnetic print table can be used with a metallic squeeze, as shown in Fig. 1. In these printing tables, an

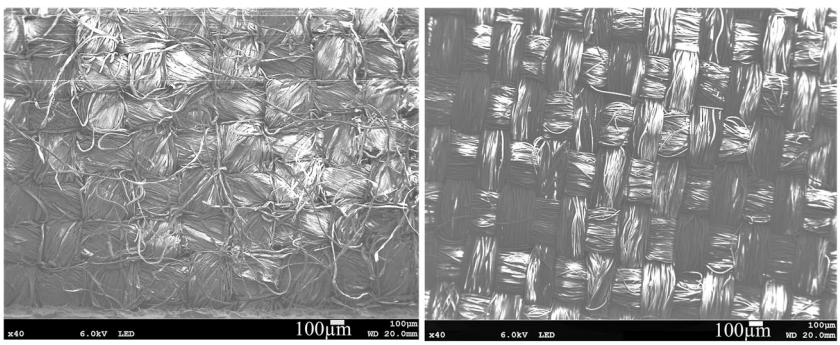

(a) (b)

Fig. 2 SEM images of different textile substrates **a** 100% cotton and **b** 100% polyester

Table 2 Properties of different textile substrates

Textile substrates	Density (g/m^2)	Thickness (mm)	Air permeability (l/m^2/s at 20 cm^2 test area)	No. of warp yarns per inch	No. of weft yarns per inch
100% cotton	118.7 ± 3.04	0.265 ± 0.010	24.68 ± 1.16	64 ± 0.63	58 ± 0.76
100% polyester	90.2 ± 2.24	0.169 ± 0.006	28.84 ± 1.42	82 ± 0.52	74 ± 0.61

Information source: experiments

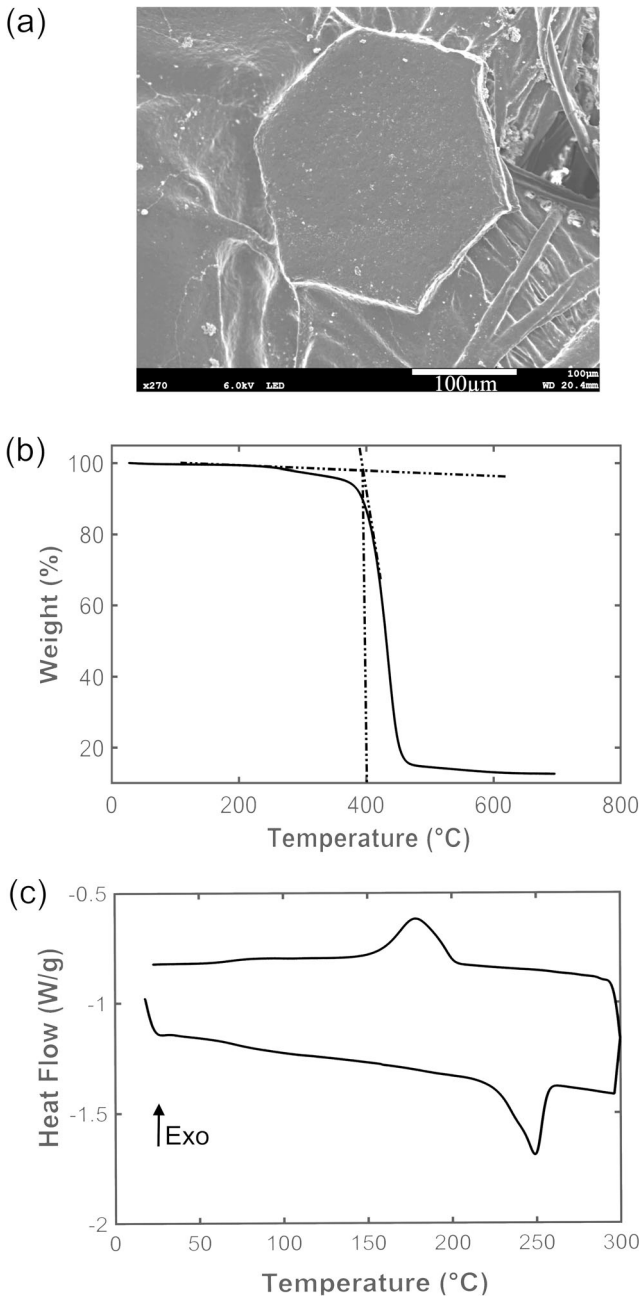

Fig. 3 **a** SEM image of micro particle (glitter) printed on the textile substrate. **b** Thermogravimetric analysis graph, **c** Differential scanning calorimetry analysis graph

electromagnetic bar that moves along the length controls the movement of the metallic squeeze and thus the squeezing pressure. Due to the transparent binder, the dark microparticles can be clearly seen on the surface of a light textile substrate after curing. While printing, these particles were enclosed within a black rectangular boundary to distinguish the printed portion and enable easy detection through a camera, as shown in Fig. 1. It can be further noted that unlike usual screen printing—that requires stencil design modification for each new motif—secured tag printing required a screen with a single square stencil of approximate size 3 × 3 cm^2 (printing area), which can be reused multiple times.

3 Materials and methods

3.1 Materials

3.1.1 Binders

Three types of commercially available binders were used in this study and standard recipes were followed to develop the final printing paste. The detailed description of the binders and curing conditions can be found in Table 1.

3.1.2 Textile substrates

Two widely used textile compositions (100% cotton and 100% polyester) for clothing application were selected in plain woven structure as the textile substrates for secured tag

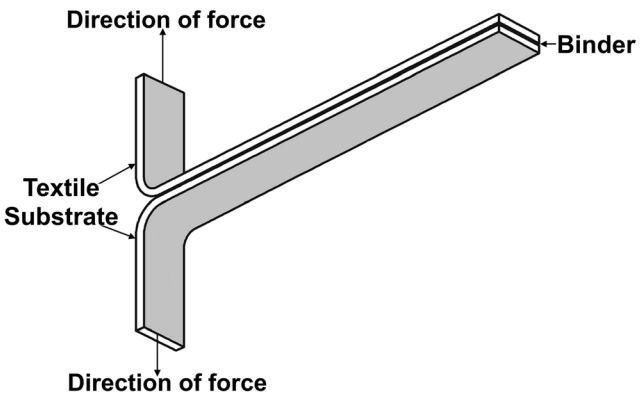

Fig. 4 Peel test specimen

Table 3 Printing paste deposition on different substrates using different printing screens

Textile substrates	Printing paste deposition rate *(g/m²)*		
	Binder 1	Binder 2	Binder 3
Cotton 10	99	205	24
Cotton 24	70	133	12
Polyester 10	86	176	21
Polyester 24	65	132	11

development. Cotton textile substrate—made up of yarns having stable fibers—had a rough and irregular surface whereas polyester textile substrate—made of continuous filament yarns—had a comparatively smoother and regular surface. Scanning electron microscope (SEM) images of the two surfaces are shown in Fig. 2 and detailed characteristics can be found in Table 2.

3.1.3 Microparticles

The printing paste also includes microparticles that are mixed with the binder, along with fixing agents, in a predefined concentration. Commercially available black Geoshine® polyester glitter (supplied by Geotech International B. V, Haarlem, Netherlands [35]) were used as microparticle. As per information provided by the supplier, these glitter particles are suitable for textile coating/printing application with high brilliance, lightfast, solvent-resistant and non-toxicity. From a wide range of sizes offered by the company, hexagonal glitter particles with an average diameter of 200 μm (Fig. 3a) were

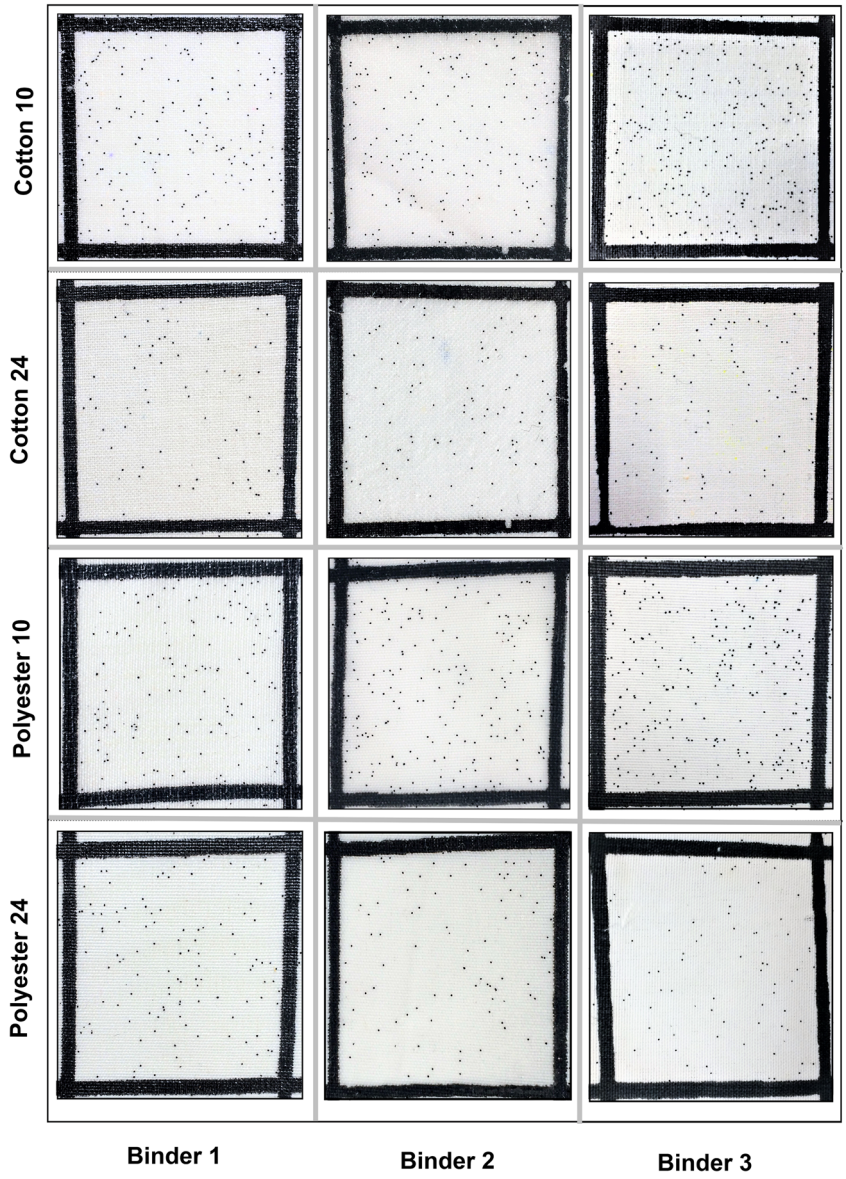

Fig. 5 Images of different printed tags

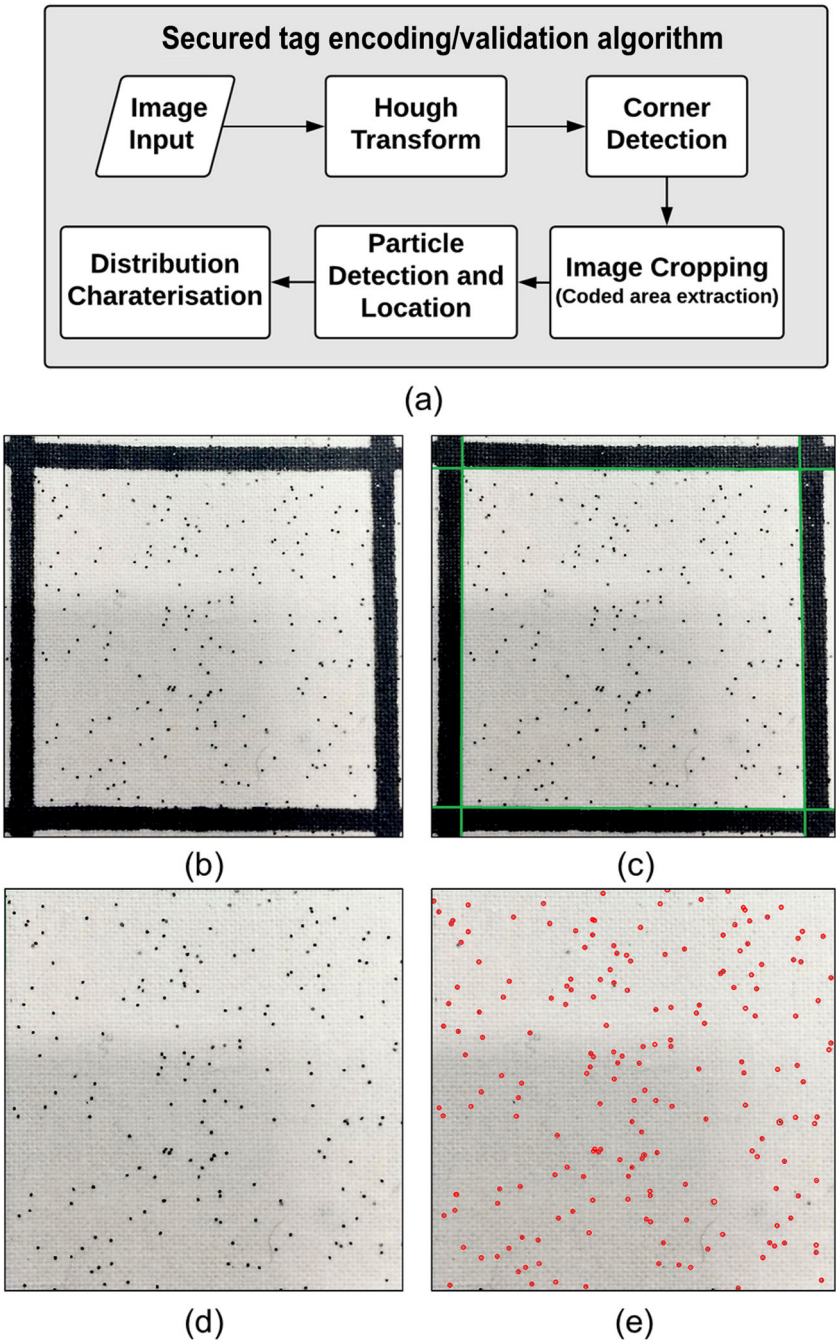

Fig. 6 **a** Secured tag encoding algorithm. **b**–**e** Different stages of particle detection. **b** Original tag image. **c** Line and corner detection. **d** Area of interest (actual tag area). **e** Particle detection

sourced for secured tag development. The size was appropriate, as it is not big and can easily be printed on the textile surface with screen printing, using screens of size 10 to 24 threads/cm. Bigger particles can block the screen mesh or would require a courser screen—resulting in high deposition and low print precision. On the other hand, smaller particles can be hard to detect by normal low-resolution cameras and would increase the processing time.

Further, the glitter particles were subjected to thermogravimetric (TG) and differential scanning calorimetry (DSC) analysis. A TG analysis was carried out using thermal analysis (TA) universal instrument, under a constant stream of nitrogen. Four independent experiments were conducted on 10.0 ± 0.1 mg samples with a heating rate of 10 °C/min starting from 0 to 750 °C. Figure 3b shows the graph of TG analysis wherein the particles were found to be thermally stable with a degradation temperature higher than 400 °C. For DSC analysis, TA instrument type DSC 2920 was used. The analysis was done under a constant stream of nitrogen on 6.0 ± 0.1 mg samples at a

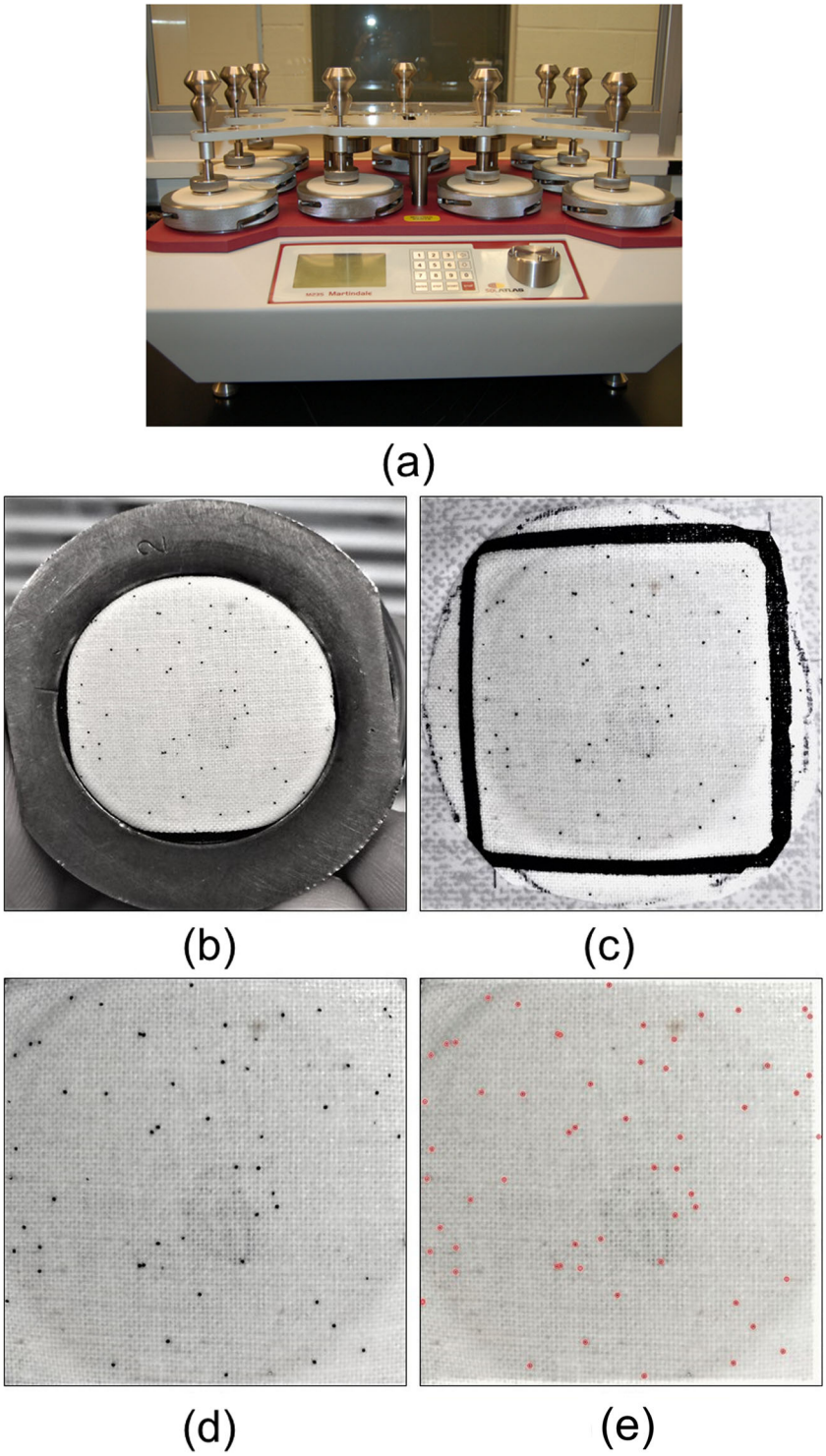

Fig. 7 **a** Martindale abrasion tester. **b** Tag mounted on the ring. **c** After abrasion cycle. **d, e** Tag area and particle detection to evaluate particle erosion

heating rate of 10 °C/min starting from 0 to 300 °C, then isotherm of 3 min followed by cooling at the same rate until 0 °C. The cycle was repeated again and the data from the second cycle was analysed and presented in Fig. 3c (DSC analysis graph), that characterises the thermal transition of the particles. These analyses show that the particles are suitable for textile printing application as they can withstand high temperature without degrading during the curing process of the binders, i.e. usually between 130 and 170 °C (as shown in Table 1).

Table 4 Results from the capillary rise and sessile drop experiments

Material	Contact angle (°)		Surface tension (mN/m)	
	Water	Diiodomethane	Dispersive	Polar
Cotton textile substrate	68.9	54.1	52.6	4.8
Polyester textile substrate	66.2	49.6	55.7	5.2
Binder 1	66.4	48.6	55.7	5.1
Binder 2	100.6	83.4	16.1	2.3
Binder 3	86.8	48.6	22.3	5.2

3.2 Methods

3.2.1 Methods for material characterisation

After material selection and characterisation, it is important to test the surface interaction and adhesion characteristics of the binders and the textile substrates. To do so, work of adhesion and peel resistance were calculated—that are important parameters for predicting the durability of the binder at the surface.

Work of adhesion is one of the non-destructive tests to measure the contact strength or work required to separate two adjacent phase boundary. It is an important parameter particularly for processes including coating, printing and bonding in order to determine the surface-surface interaction and adhesion force. According to the thermodynamic mechanism of adhesion, the polymer system, in a neutral environment (like air) attempts to reduce the surface free energy by aligning the surface into non-polar regions of the polymer. The interfacial tension between polymer surface and polar substance (such as water) in contact minimises in case of a good adhesion system. Based on the concept, Young [36] formulated a relation for the strength of adhesion of a simple system that can be estimated through the work of adhesion(W_a). The formulated relation uses a liquid of known surface tension (γ_L) that is in contact with simple solid, smooth, isotropic and non-deformable surface and defines work of adhesion as

$$W_a = \gamma_S + \gamma_L - \gamma_{SL} \tag{1}$$

$$\gamma_L \cos\theta = \gamma_S - \gamma_{SL} \tag{2}$$

where γ_S = surface tension solid/air, γ_L= surface tension liquid/air, γ_{SL}= surface tension solid/liquid and θ = contact angle between solid and liquid surface.

However, in the above equations, even after knowing γ_L, there are other unknown variables. Therefore, to determine the work of adhesion between the binders and the textile substrates, we use the OWRK methods named after the originators Owens, Wendt, Rebel and Kaelble [37]. It is an extension of Fowkes' model [38] that considers the influence of both polar (γ^p) (hydrogen bonding) and dispersive (γ^d) components (all the van der Waals forces) and takes their geometric mean to calculate the surface free energy as:

$$\gamma_{SL} = \gamma_S + \gamma_L - 2\sqrt{\gamma_S^d \gamma_L^d} - 2\sqrt{\gamma_S^p \gamma_L^p} \tag{3}$$

And by combining Eqs. (2) and (3)

$$\gamma_L(1+\cos\theta) = 2\sqrt{\gamma_S^d \gamma_L^d} + 2\sqrt{\gamma_S^p \gamma_L^p}, \tag{4}$$

And combining Eqs. (1) and (3)

$$W_a = 2\sqrt{\gamma_S^d \gamma_L^d} + 2\sqrt{\gamma_S^p \gamma_L^p} \tag{5}$$

In this study, using Eq. (4) and the method used by [39], the work of adhesion value has been calculated for different textile substrates and binders. Using two known liquids with different polarity (water and diiodomethane) whereas contact angle between the known liquids/binders (through sessile drop technique) and known liquids/textile substrates (through capillary rise method) has been measured in separate tests. These values served as input for Eq. 5 to calculate the work of adhesion.

Peel test is a destructive test method for direct adhesion measurement. It calculates the forces required to tear, break and delaminate adhered layers by peeling. In this study, we follow ISO 24345:2006 testing protocols to determine peel resistance. MTS tensile testing machine, capable to maintain test speed and provide appropriate load, has been used. Six bonded samples consisting of two types of textile substrates with three type of binders were developed for the test. Further, six test specimens—three each from the warp and weft directions of each samples with 150-mm long and 50-mm width—were cut at a regular distance at least 100 mm away from the edges. These samples were condensed at 23 ± 2 °C temperature and 50 ± 5% relative humidity for 24 h before the test. Each specimen (as shown in Fig. 4) was placed in jaws of tensile tester (around 50 mm apart), and the jaws were separated by a speed of 100 ± 5 mm/min and separation force (peel resistance) is recorded.

3.2.2 Methods for secured tag analysis

As discussed earlier, the secured tag was printed using screen printing process. Therefore, to examine the variation in print durability and readability, two types of screens—with mesh size 10 threads/cm and 24 threads/cm were used for secured tag development. Screen with mesh size 10 threads/cm has courser mesh or larger holes, which should allow more paste (along with particle) to squeeze through the screen as compared to 24 threads/cm. This results in higher paste deposition and more particle concentration in the printed area. The print deposition rates obtained through both screens on different textiles are shown in Table 3 and corresponding images of the tags are shown in Fig. 5. It should be noted that the 100% cotton textile substrate samples printed using a screen with 10 threads/cm mesh size are referred as 'Cotton 10' and likewise, 'Cotton 24', 'Polyester 10' and 'Polyester 24' denote the type of textile substrate and screen mesh size.

Tag encoding and validation mechanism In order to detect the printed particles, a digital image of each secured tag was captured and processed using image processing and pattern recognition algorithm on Matlab R2017b. The main steps of the algorithm to detect and extract the particle locations are shown in Fig. 6a, followed by a pictorial representation of the same using image of a unique secured tag in Fig. 6b–e. It should be noted that the same steps for particle detection would be followed during encoding as well as the validation stages. The image was first pre-processed to correct the contrast and light. Then, the Hough transform [40] was applied to detect the lines, tag corners and ultimately the secured tag area with random particle distribution. The resultant area was then cropped and particles were detected and located using Circular Hough transformation [40]. Using these particles, location features like the strong cluster of particles and empty areas in the secured tag were extracted and encoded in form of unique traceability code. Further, a fuzzy membership-based validation algorithm has been developed considering the flexible nature of the textile substrate and abrasion that it might undergo during the use phase. A detailed explanation of the algorithm can be found in our previous work [31]. As demonstrated in [31], the algorithm showed positive results with correct validation of authentic secured tag even after 20% particle erosions from the surface. In order to analyse the durability of the secured tag, images of the developed tag samples are taken at different stages, i.e. after print and after each wash/abrasion cycle. The obtained images are analysed using the image-processing algorithm to quantify particle erosion.

Washing test The samples were washed 10 times following ISO 6300:2015 washing test procedure. Each wash-cycle comprises of 30 min of washing at 60 °C temperature in a mixture of European Colourfastness Establishment (ECE) normalised detergent and water (0.5% *w*/*w* of detergent) followed by line drying. After each wash, images of the secured tag were captured and analysed using the image-processing algorithm, as explained in the previous section, to count the percentage of particle erosion.

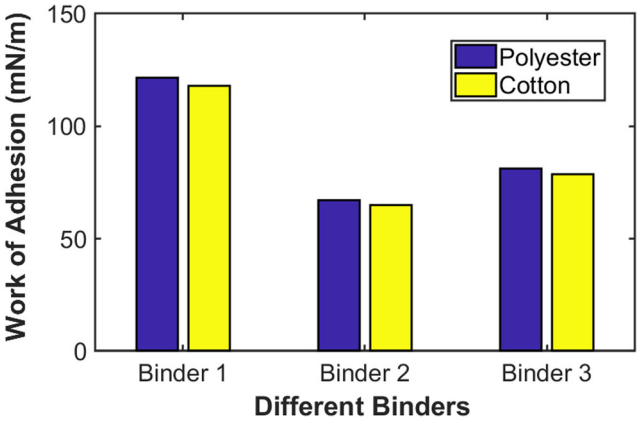

Fig. 8 Work of adhesion for different binders

Abrasion test In order to test the abrasion resistance, the developed samples were tested as per the ASTM D4966 test procedure using Martindale abrasion tester as shown in Fig. 7a.

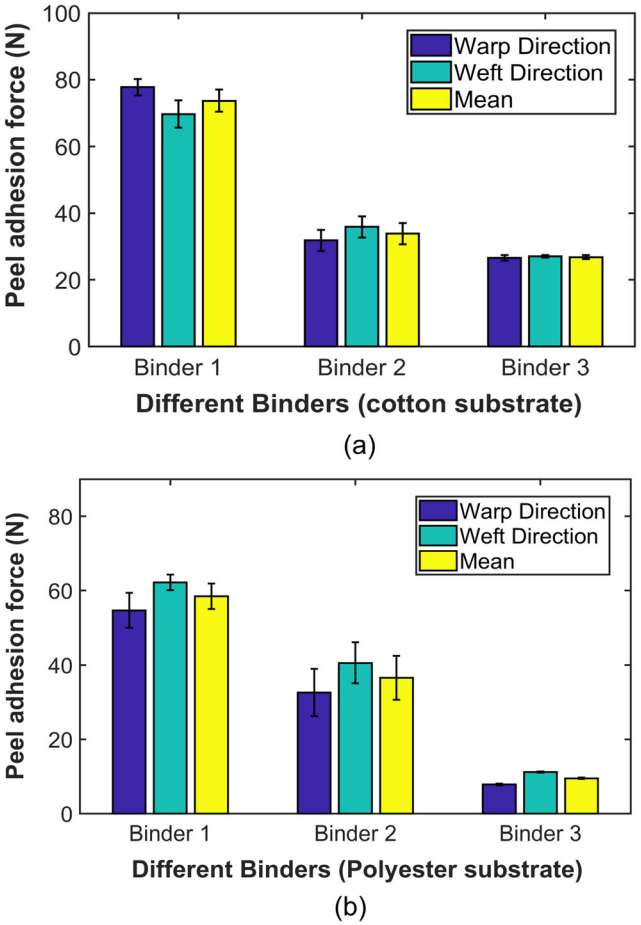

Fig. 9 Peel adhesion force (N) for the different binders with **a** cotton textile substrate and **b** polyester textile substrate

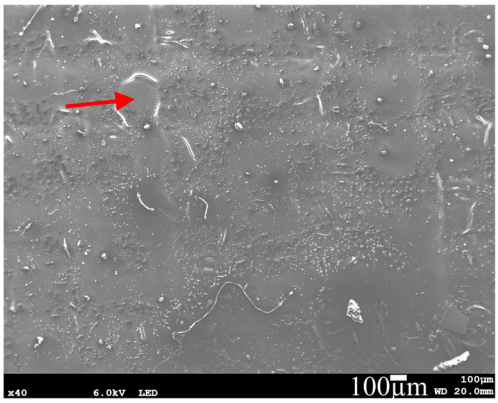

Fig. 10 SEM image of polyester 24 printed with Binder 1

During the test, circular specimen (38-mm diameter) of each sample tag, backed by a polyurethane foam is mounted on a ring. The ring performs a Lissajous motion against a standard wool abradant textile with the face side of the tag in contact with the abradant. In order to observe the particle erosion, images of the tag specimens were taken and analysed using the image processing as shown in Fig. 7b–e, at 0, 500, 750, 1000, 2500, 5000 and 7500 abrasion cycles.

SEM analysis Scanning electron microscopy is a widely used surface investigation technique that uses electron scattering to map the surface topography. In this method, an electron beam is rastered across the conductive surface (usually made conductive by coating with a conductive material) of the sample. An electron detector records secondary electron emitted signals generated during electron rastering that develops the image of the sample. SEM has a high depth of field compared to an optical microscope and can generate images with few nanometres spatial resolutions. Topographical information provided by SEM analysis has been used to analyse the interaction between the substrates and printing paste before and after wash cycles.

Surface roughness analysis—profilometer In order to quantify surface roughness and surface profile of the prepared samples at different stages, the samples were subjected to a profilometer test. It consists of mainly two parts. Detector or stylus that moves and physically sense the surface of the specimen that is mounted over the sample stage that holds the specimen. The stylus in conjunction with a feedback loop physically moves over the specimen surface while maintaining a constant force to acquire surface height and roughness information along the scan line. Various ISO 25178 surface texture height parameters—the arithmetic mean height (Sa), root mean square height (Sq), maximum peak height (Sp) and maximum pit height (Sv) were evaluated for each sample using the equipment.

4 Results and discussion

4.1 Results of material characterisation

4.1.1 Work of adhesion value

Due to the hydrophilic nature of the two textile substrates (cotton and polyester), the contact angle and the surface tension has been calculated using the tensiometric method. Whereas, sessile drop technique was used for calculating the

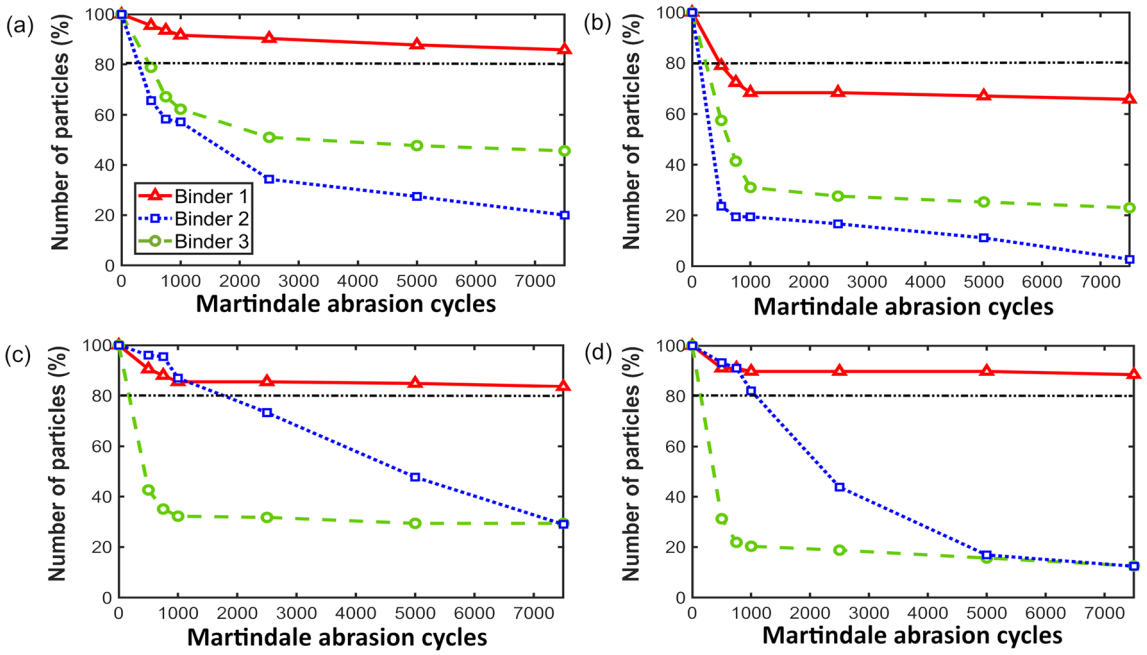

Fig. 11 Abrasion resistance test results. **a** Cotton 10. **b** Cotton 24. **c** Polyester 10. **d** Polyester 24

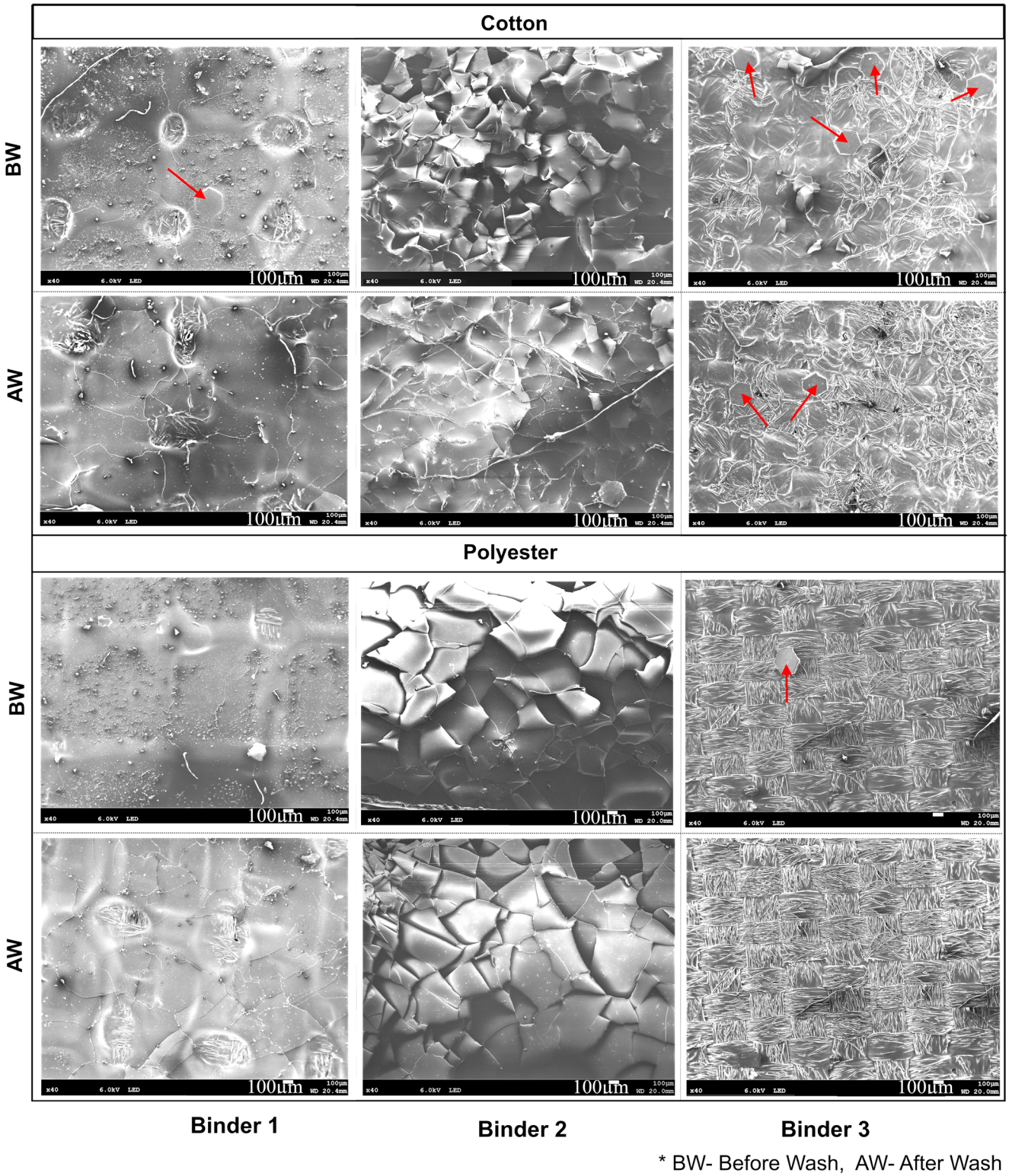

Fig. 12 SEM images of the surface of textile substrates after screen printing, before and after wash

surface tension of binders. Table 4 summarises the results from these experiments.

Values from Table 4 were combined to get the work of adhesion (W_a) between different binders and textile substrates. It can also be inferred from Fig. 8 that although made from different materials (cotton and polyester), the surfaces of textile substrates have similar surface tension values and were behaving alike with the same binder.

Besides the surface roughness parameters calculated from profilometer for both textile substrates were also very similar with (Sa, Sq) = (0.020, 0.056) for cotton and (0.023, 0.029) for polyester (refer Appendix Table 6 for detail). The $W_a$value for binder 1 (vinyl acrylic copolymer) was found to be highest with a value of 121.7 mN/m with the polyester textile substrate and 118.1 mN/m with the cotton textile substrate. As explained above, according to the thermodynamic mechanism of adhesion, polymer system, in a neutral environment (like air) attempts to reduce the surface free energy by aligning the surface into non-polar regions of the polymer. In case of the polymer textile substrate and binder 1 the surface tension value is almost equal and comparatively higher than others material; hence, they combine to form an equilibrium at the interface and high adhesion [41]. Binder 3 (styrene acrylic copolymer) has the second highest W_a value, 81.0 mN/m with the polyester textile substrate and 78. 6mN/m with the cotton textile substrate. Finally, we obtained the lowest W_a for binder 2 (silicones) as 67.0 mN/m with the polyester textile substrate and 65.0 mN/m with the cotton textile substrate. These can be due to a comparatively high difference between the surface tension of the binder 2 and the textile substrates (refer Table 4).

4.1.2 Peel resistance values

Test specimens were placed between the jaws of the tensile tester approximately 50 mm apart, one at a time. The recording device continuously recorded the peeling or separation force at a separation speed of 100 ± 5 mm/min. Mean value of the peel resistance (force) is calculated (rounded to nearest 5 N) throughout the peeling process, neglecting the reading from first and the last quarter of the total reading.

Results of the peel test experiment as shown in Fig. 9, indicate that binder 1 has the highest peel adhesion force value for both types of textile substrates with a mean values of 73.75 N (for cotton) and 58.44 N (for polyester). This is followed By Binder 2 that has a mean values of 33.86 N for cotton textile substrate and 36.62 N for the polyester textile substrate. Finally, binder 3 has shown the lowest peel adhesion force with polyester textile substrate equal to 9.55 N and slightly higher value of 26.79 N for the cotton textile substrate. Unlike the work of adhesion value, binder 2 has a slightly higher peel resistance compared to binder 3. The possible answer to this behavior can be the low solid content (38%) of binder 3 compared to binder 2, which has 100% solid content. On the other hand, vinyl acrylic copolymer-based binder 1 had around 60% solid contact and also (OH) group that shows high affinity with cellulosic fibre (cotton textile substrate), thus resulting in highest peel resistance value.

After experimental adhesion characterisation, secured tag samples were printed, using binders (mixed with microparticle) on the textile substrates. These samples were tested for abrasion and wash durability along with surface interaction investigation using SEM images.

4.2 Results of secured tag analysis

4.2.1 Abrasion resistance value

In case of abrasion resistance test, secured tag samples printed with binder 1 using a screen of mesh size of 10 threads/cm on both textile substrates (cotton and polyester) and mesh size of 24 threads/cm on polyester, proved to be the most durable. They could withstand 7500 abrasion cycle with an erosion

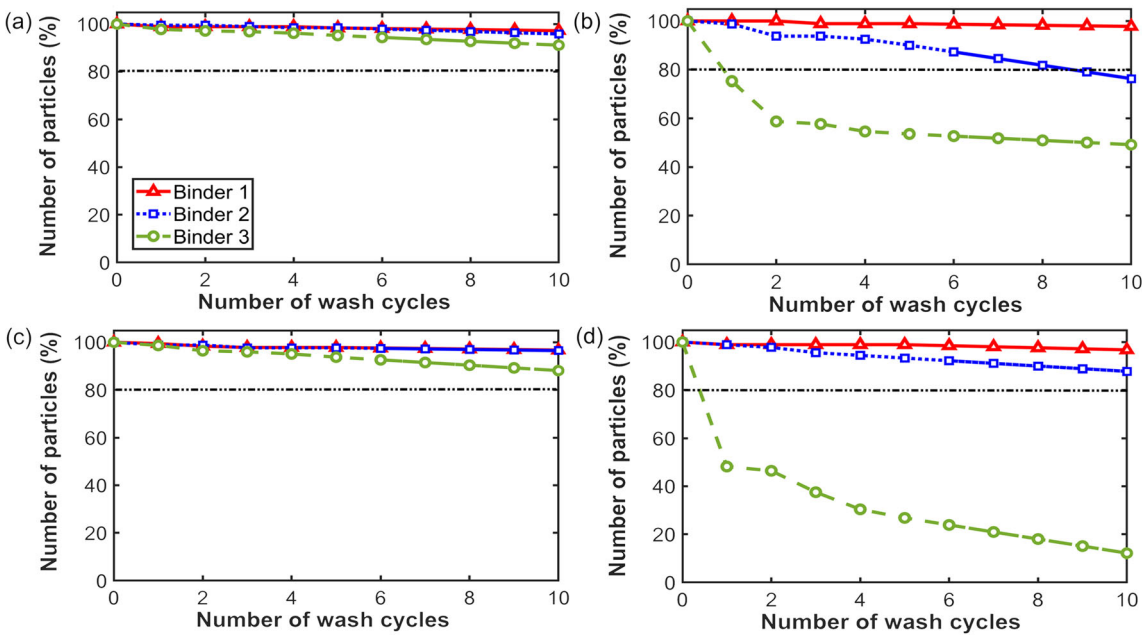

Fig. 13 Washing test results. **a** Cotton 10. **b** Cotton 24. **c** Polyester 10. **d** Polyester 24

Table 5 Result summary: a comparative analysis (I = first rank, II = second rank and III = third rank)

Binder	Textile substrates and screen type	Work of adhesion	Peel adhesion force	Abrasion test	Washing test
Binder 1	Cotton 10	I	I	I	I
	Cotton 24			II	I
	Polyester 10	I	I	I	I
	Polyester 24			I	I
Binder 2	Cotton 10	III	II	III	I
	Cotton 24			III	II
	Polyester10	III	II	II	I
	Polyester 24			II	I
Binder 3	Cotton 10	II	III	II	I
	Cotton 24			II	III
	Polyester10	II	III	III	I
	Polyester 24			III	III

of less than 20% of the total particles. This proves that the secured tag, when printed with binder 1, can withstand high abrasion. The secured tag will be durable when printed on the similar textile substrate and can be validated successfully without hampering the code (or random particle distribution). In fact, polyester 24, although printed with a lower rate of binder deposition was durable against abrasion. A further investigation using SEM image (as shown in Fig. 10) shows the possible reason to be the smooth and even deposition of binder (with low friction) on the surface of polyester and the cotton textile substrate. The binder seems to have completely covered the particle, preventing it from possible exposure to the abradant. Detailed abrasion resistance results for all type of binders and substrates are shown in Fig. 11. Binder 2 was found to be less durable against abrasion due to the scaly and rough surface formed on the textile substrate after print—that can be observed in Fig. 12.

4.2.2 Wash test results

In the case of wash test, secured tag samples printed with combinations of cotton 10 or polyester 10 with all the three types of binders showed good resistance to washing. These samples withstood 10 wash cycles with particle erosion as low as 2% for binder 1 and around 10% for binders 2 and 3. In case of cotton 24 and polyester 24 due to the lower rate of binder deposition, the wash durability was found to slightly lower for binder 1 and binder 2 and very low for binder 3. Figure 13 graphically represents the number of particles (in percentage) remaining on individual secured tag sample after each wash cycle.

Figure 12 further shows the SEM analysis (surface interaction) of these samples before and after wash. In accordance with the wash test results, the images indicate the reasons for the low durability of a certain binder. For example, in the case of binder 3, the particles are not completely covered with printing paste and visible on the surface of the textile substrate. This results in easy erosion of micro-particle during washing and surface abrasion, resulting in lower durability. Similarly, made with hydrophobic silicon material, binder 2 has a good wash resistance. Values from the profilometer analysis of different samples can be found in Appendix Table 6 that further indicates the possible reasons for low durability among the samples.

Finally, Table 5 summarises all the results and presents a comparative analysis of different binders and textile substrates. It ranks different samples based on their performance in comparison to others, taking into consideration the 20% threshold values for particle erosion (under which the secured tag code would work successfully). It can be observed that secured tag samples that were printed with binder 1 using a screen of mesh size 10 threads/cm give the best results for both the textile substrates in all the different durability tests. For the polyester substrate, a secured tag can even be printed using a screen of mesh size 24 threads/cm, which showed a high durability against washing and abrasion.

5 Conclusions

The study presents a new secured tag for textile product authentication and traceability in T&C supply chain. The secured tag is realised by printing randomly distributed microparticles on the textile surface through an uncontrolled screen printing mechanism. Thus, the obtained randomness in particle distribution is unclonable and acts like a unique signature for each product. In addition, this secured tag can be easily read and verified using a smartphone camera, thereby imparting additional functionality

to the textiles. The study systematically explains the development process of the secured tag (including design, fabrication and encoding/validation algorithm) followed by an in-depth investigation of different raw materials (in form of three binders and two textile substrates) and their interaction. Tests such as abrasion and wash resistance have also been performed to examine the durability and readability of the tag during textile use phase. Finally, all results were compared to determine the optimum combination.

It has been observed that secured tag printed with binder 1 (vinyl acrylic copolymer) performs best among all performed tests, whereas binder 2 (silicones) performed better in wash resistance. On the other hand, binder 3 (styrene acrylic copolymer) does not prove appropriate for the secured tag fabrication. Since the performed tests simulate the real-use condition of garments, therefore, it is anticipated that the fabricated tags can sustain the various use conditions of textile.

It should be noted that the current study is a proof-of-concept of a new traceability tag. Therefore, for the initial experimental validation, two widely used textile substrates (100% cotton and 100% polyester) with relatively stable woven structure were selected. In the future, different fibre blends and textile structures (including knits and nonwovens) will be selected for experimental validation. The tags can be further tested for dry cleaning and other chemical cleaning processes. Future study can also focus on lifecycle analysis of binders 1 and 2 to explore the most sustainable alternative. A piloting of the developed system in real industrial scenarios would be the next step to explore further challenges and their solutions at the manufacturing stage.

Acknowledgments The authors would like to thank Mr. Christian Catel from ENSAIT/GEMTEX, France, for his time and help.

Funding This work has been comprehended in the framework of Erasmus Mundus Joint Doctorate Project—SMDTex (Sustainable Management and Design for Textiles), which is financed by the European Commission.

Appendix

Table 6 Profilometer reading for different specimen

Adhesive type	Treatment	Sample	Sa	Sq	Sp	Sv
No binder	Before wash	Cotton	0.0203	0.0256	0.209	0.0132
		Polyester	0.0237	0.0294	0.123	0.112
Binder1	Before wash	Cotton10	0.038	0.051	0.252	0.178
		Polyester 10	0.0361	0.0467	0.358	0.181
		Cotton 24	0.0426	0.0511	0.217	0.176
		Polyester 24	0.0286	0.0383	0.265	0.114
	After wash	Cotton 10	0.0362	0.0454	0.204	0.196
		Polyester 10	0.0292	0.0371	0.18	0.175
		Cotton 24	0.0532	0.0679	0.322	0.185
		Polyester 24	0.0381	0.0501	0.235	0.135
Binder2	Before wash	Cotton10	0.0449	0.0555	0.272	0.156
		Polyester 10	0.0302	0.0356	0.178	0.0873
		Cotton 24	0.0259	0.0332	0.248	0.125
		Polyester 24	0.0283	0.0334	0.155	0.0949
	After wash	Cotton 10	0.0395	0.0499	0.255	0.146
		Polyester 10	0.0351	0.0492	0.238	0.117
		Cotton 24	0.0481	0.0615	0.285	0.215
		Polyester 24	0.0232	0.029	0.134	0.14
Binder3	Before wash	Cotton 10	0.0727	0.0888	0.33	0.212
		Polyester 10	0.0421	0.0516	0.184	0.172
		Cotton 24	0.077	0.0911	0.336	0.191
		Polyester 24	0.0285	0.0362	0.164	0.125
	After wash	Cotton 10	0.0642	0.0801	0.295	0.25
		Polyester 10	0.0433	0.0522	0.152	0.169
		Cotton 24	0.0386	0.0497	0.239	0.159
		Polyester 24	0.0417	0.0506	0.181	0.151

References

1. Gupta D (2011) Functional clothing—definition and classification. Indian J Fibre Text Res 36:321–326
2. Agrawal TK, Thomassey S, Cochrane C, Lemort G, Koncar V (2017) Low-cost intelligent carpet system for footstep detection. IEEE Sensors J 17:4239–4247. https://doi.org/10.1109/JSEN.2017.2703633
3. Kelly FM, Meunier L, Cochrane C, Koncar V (2013) Polyaniline: application as solid state electrochromic in a flexible textile display. Displays 34:1–7. https://doi.org/10.1016/j.displa.2012.10.001
4. Bahadir MC, Bahadir SK (2015) Selection of appropriate e-textile structure manufacturing process prior to sensor integration using AHP. Int J Adv Manuf Technol 76:1719–1730. https://doi.org/10.1007/s00170-014-6399-x
5. Chen Y, Ge F, Guang S, Cai Z (2018) Low-cost and large-scale flexible SERS-cotton fabric as a wipe substrate for surface trace analysis. Appl Surf Sci 436:111–116. https://doi.org/10.1016/j.apsusc.2017.11.288
6. Pulit-Prociak J, Chwastowski J, Kucharski A, Banach M (2016) Functionalization of textiles with silver and zinc oxide nanoparticles. Appl Surf Sci 385:543–553. https://doi.org/10.1016/j.apsusc.2016.05.167
7. Morent R, De Geyter N (2011) Improved textile functionality through surface modifications. In: Pan N, Sun G (eds) Functional textiles for improved performance, protection and health. Woodhead Publishing, pp 3–26
8. Cao J, Huang Z, Wang C (2018) Natural printed silk substrate circuit fabricated via surface modification using one step thermal transfer and reduction graphene oxide. Appl Surf Sci 440:177–185. https://doi.org/10.1016/j.apsusc.2018.01.094
9. Oner M, Ustundag A, Budak A (2017) An RFID-based tracking system for denim production processes. Int J Adv Manuf Technol 90:591–604. https://doi.org/10.1007/s00170-016-9385-7
10. Merilampi SL, Björninen T, Ukkonen L, Ruuskanen P, Sydänheimo L (2011) Characterization of UHF RFID tags fabricated directly on convex surfaces by pad printing. Int J Adv Manuf Technol 53:577–591. https://doi.org/10.1007/s00170-010-2869-y
11. Weremczuk J, Tarapata G, Jachowicz R (2012) Humidity sensor printed on textile with use of ink-jet technology. Procedia Eng 47:1366–1369. https://doi.org/10.1016/j.proeng.2012.09.410
12. Yang K, Freeman C, Torah R, Beeby S, Tudor J (2014) Screen printed fabric electrode array for wearable functional electrical stimulation. Sensors Actuators A Phys 213:108–115. https://doi.org/10.1016/j.sna.2014.03.025
13. Street RA, Ng TN, Schwartz DE, Whiting GL, Lu JP, Bringans RD, Veres J (2015) From printed transistors to printed smart systems. Proc IEEE 103:607–618. https://doi.org/10.1109/JPROC.2015.2408552
14. Locher I, Tröster G (2007) Screen-printed textile transmission lines. Text Res J 77:837–842. https://doi.org/10.1177/0040517507080679
15. Little AF, Christie RM (2010) Textile applications of photochromic dyes. Part 2: factors affecting the photocoloration of textiles screen-printed with commercial photochromic dyes. Color Technol 126:164–170. https://doi.org/10.1111/j.1478-4408.2010.00242.x
16. Abe T (2012) Present state of inkjet printing technology for textile. Adv Mater Res 441:23–27. https://doi.org/10.4028/www.scientific.net/AMR.441.23
17. Huang SH, Liu P, Mokasdar A, Hou L (2013) Additive manufacturing and its societal impact: a literature review. Int J Adv Manuf Technol 67:1191–1203. https://doi.org/10.1007/s00170-012-4558-5
18. Cherenack K, van Pieterson L (2012) Smart textiles: challenges and opportunities. J Appl Phys 112:091301. https://doi.org/10.1063/1.4742728
19. Guan Y, Hu J, Li Y, Ma W, Zheng Y (2011) A new anti-counterfeiting method: fluorescent labeling by safranine T in tobacco seed. Acta Physiol Plant 33:1271–1276. https://doi.org/10.1007/s11738-010-0657-9
20. Hu H, Chen Q-W, Tang J, Hu XY, Zhou XH (2012) Photonic anti-counterfeiting using structural colors derived from magnetic-responsive photonic crystals with double photonic bandgap heterostructures. J Mater Chem 22:11048–11053. https://doi.org/10.1039/C2JM30169E
21. Ilie-Zudor E, Kemény Z, van Blommestein F, Monostori L, van der Meulen A (2011) A survey of applications and requirements of unique identification systems and RFID techniques. Comput Ind 62:227–252. https://doi.org/10.1016/j.compind.2010.10.004
22. Kumar V, Koehl L, Zeng X, Ekwall D (2017) Coded yarn based tag for tracking textile supply chain. J Manuf Syst 42:124–139. https://doi.org/10.1016/j.jmsy.2016.11.008
23. Cui Y, Phang IY, Lee YH, Lee MR, Zhang Q, Ling XY (2015) Multiplex plasmonic anti-counterfeiting security labels based on surface-enhanced Raman scattering. Chem Commun Camb Engl 51:5363–5366. https://doi.org/10.1039/c4cc08596e
24. Bansal D, Malla S, Gudala K, Tiwari P (2013) Anti-counterfeit technologies: a pharmaceutical industry perspective. Sci Pharm 81:1–13. https://doi.org/10.3797/scipharm.1202-03
25. Seino K, Kuwabara S, Mikami S, et al (2004) Development of the traceability system which secures the safety of fishery products using the QR code and a digital signature. In: Oceans '04. Mtts/IEEE Techno-Ocean '04. pp 476–481
26. Sowade E, Göthel F, Zichner R, Baumann RR (2015) Inkjet printing of UHF antennas on corrugated cardboards for packaging applications. Appl Surf Sci 332:500–506. https://doi.org/10.1016/j.apsusc.2015.01.113
27. Strickland LS, Hunt LE (2005) Technology, security, and individual privacy: new tools, new threats, and new public perceptions. J Am Soc Inf Sci Technol 56:221–234. https://doi.org/10.1002/asi.20122
28. Kumar V, Koehl L, Zeng X (2016) A fully yarn integrated tag for tracking the international textile supply chain. J Manuf Syst 40:76–86. https://doi.org/10.1016/j.jmsy.2016.06.007
29. Luttropp C, Johansson J (2010) Improved recycling with life cycle information tagged to the product. J Clean Prod 18:346–354. https://doi.org/10.1016/j.jclepro.2009.10.023
30. Devadas S, Suh E, Paral S, et al (2008) Design and implementation of PUF-based "Unclonable" RFID ICs for anti-counterfeiting and security applications. In: 2008 IEEE international conference on RFID. pp 58–64
31. Agrawal TK, Koehl L, Campagne C (2018) A secured tag for implementation of traceability in textile and clothing supply chain. Int J Adv Manuf Technol 99:2563–2577. https://doi.org/10.1007/s00170-018-2638-x
32. Product - CHT group - special chemicals. https://www.cht.com/cht/web.nsf/id/pa_en_productdetail.html?Open&pID=00039825.108_EN. Accessed 4 Jun 2018

33. Coating silicone SILBIONE TCS 7541 A | Elkem Silicones. https://silicones.elkem.com/EN/our_offer/Product/90060757/90060758/SILBIONE-TCS-7541-A. Accessed 20 Nov 2018
34. Archroma coatings, adhesives & sealants. http://www.cas.archroma.com/. Accessed 20 Nov 2018
35. Home. https://www.geotech.nl/en/. Accessed 20 Nov 2018
36. Young T, Peacock G, Leitch J (1855) Miscellaneous works of the late Thomas Young. J. Murray, London
37. Owens DK, Wendt RC Estimation of the surface free energy of polymers. J Appl Polym Sci 13:1741–1747. https://doi.org/10.1002/app.1969.070130815, 1969
38. Fowkes FM (1962) Determination of interfacial tensions, contact angles, and dispersion forces in surfaces by assuming additivity of intermolecular interactions in surfaces. J Phys Chem 66:382–382. https://doi.org/10.1021/j100808a524
39. Di J, Perwuelz A, Gueguen V (2001) The surface energy of PET fabrics coated with silicone. J Text Inst 92:184–192. https://doi.org/10.1080/00405000108659569
40. Duda RO, Hart PE (1972) Use of the Hough transformation to detect lines and curves in pictures. Commun ACM 15:11–15. https://doi.org/10.1145/361237.361242
41. Lipatov YS (1995) Polymer reinforcement. ChemTec Publishing